Engineering and Computational Mechanics

Optimisation of a ground anchor head for NDT monitoring

--Manuscript Draft--

Manuscript Number:	EACM-D-16-00012R2
Full Title:	Optimisation of a ground anchor head for NDT monitoring
Article Type:	Paper
Corresponding Author:	A Ivanovic Fraser Nobel Building Aberdeen, Scotland UNITED KINGDOM
Corresponding Author Secondary Information:	
Corresponding Author's Institution:	Fraser Nobel Building
Corresponding Author's Secondary Institution:	
First Author:	Ana Ivanovic, Ph.D
First Author Secondary Information:	
Order of Authors:	Ana Ivanovic, Ph.D
	Alberto Monese
	Richard D Neilson, PhD
Order of Authors Secondary Information:	
Abstract:	Ground anchorages and rock bolts are used widely in retaining walls, mines, dry docks, dams and pre-stressed structures to provide effective support for unstable rock strata. The non-destructive Ground Anchorage Integrity Testing (GRANIT) method has been used commercially to monitor the load in these types of support structures. The GRANIT system detects changes in the natural frequencies of the system, and the configuration of the anchor head plays a crucial role in determining the natural frequencies associated with load assessment. When using this system, the anchor head assembly needs to have a nonlinear stiffness characteristic to permit changes in anchorage load to be detected. This paper offers a new design of the anchor head which is designed to maximise the quality of load estimation using the GRANIT system. The initial estimate of the optimal stiffness characteristic is found using a lumped parameter dynamic model of the bolt assembly. Finite element models of the proposed patented plate designs are then presented along with the corresponding load-displacement diagrams. The optimised bearing plate which was designed in this process was manufactured and tested experimentally, both statically and dynamically as part of a rock bolt assembly. The results from the experiments and from the dynamic model are presented and show good agreement and the resulting frequency shifts with the change of load prove the viability of building in the flexibility required to make non-destructive monitoring of load possible and that the proposed design provides excellent load estimation.
Funding Information:	Engineering and Physical Sciences Research Council (EP/E050301/1) — Dr Ana Ivanovic

Answers to Reviewers' comments

Title: Optimisation of a ground anchor head for NDT monitoring
Article number: EACM-D-16-00012

The nomenclature is now included reflecting symbols used in the text.

The figures are now of a higher quality – as required by the journal

The references follow the style required by the journal.

Optimisation of a ground anchor head for NDT monitoring

Ana Ivanović*, Alberto Monese, and Richard D. Neilson

School of Engineering, University of Aberdeen

*corresponding author

Ana Ivanović,
School of Engineering, University of Aberdeen
Aberdeen, AB24 3UE, United Kingdom
Tel: 01224 273265
e-mail: a.ivanovic@abdn.ac.uk

Abstract

Ground anchorages and rock bolts are used widely in retaining walls, mines, dry docks, dams and pre-stressed structures to provide effective support for unstable rock strata. The non-destructive **Gr**ound **A**nchorage **I**ntegrity **T**esting (GRANIT) method has been used commercially to monitor the load in these types of support structures. The GRANIT system detects changes in the natural frequencies of the system, and the configuration of the anchor head plays a crucial role in determining the natural frequencies associated with load assessment. When using this system, the anchor head assembly needs to have a nonlinear stiffness characteristic to permit changes in anchorage load to be detected. This paper offers a new design of the anchor head which is designed to maximise the quality of load estimation using the GRANIT system. The initial estimate of the optimal stiffness characteristic is found using a lumped parameter dynamic model of the bolt assembly. Finite element models of the proposed patented plate designs are then presented along with the corresponding load-displacement diagrams. The optimised bearing plate which was designed in this process was manufactured and tested experimentally, both statically and dynamically as part of a rock bolt assembly. The results from the experiments and from the dynamic model are presented and show good agreement and the resulting frequency shifts with the change

of load prove the viability of building in the flexibility required to make non-destructive monitoring of load possible and that the proposed design provides excellent load estimation.

Keywords: Ground anchorages, bearing plate, contact mechanics, design

List of notation

A - cross sectional area

a,b,c,d - coefficients of polynomial cubic curve

x - deflection

k_{bp} - stiffness of the bearing plate

k_{bolt} - the stiffness of the free length of the steel tendon

r - ratio between k_{bp} and k_{bolt}

l_{free}- free length

E- Young's modulus

1. Background

1.1. Introduction

Structures like mines, tunnels and retaining walls are often supported by ground anchorages and currently, millions of these are installed worldwide. Ground anchorages are capable of transmitting loads from structures to strong underlying rock or soil strata [1,2] to provide support. A number of different configurations exist depending on the application: whether in rock or soil, whether they are permanent or temporary and whether they are active (prestressed) or passive (initially not stressed). Regardless of the type of anchorage, the common parts of any anchorage system are the protruding, free and fixed anchor lengths and an anchor head assembly through which the load is transmitted to the surrounding rock/soil mass (Figure 1a). The anchor head assembly consists of a stressing nut and a bearing plate in the case of a rock bolt and a bearing plate and barrel with wedges in the case of a strand anchor. The main principle of applying the load to a bolt or cable/strand after installation is to stretch the tendon between the fixed anchorage length and the bearing plate and therefore introduce compressive loads into the rock/soil surface which in turn provide stabilization of the surrounding mass. Generally,

monitoring of such anchorages is restricted to 5-10% of installations and is undertaken by means of pull out tests [3], which are destructive, or by load cells which are too expensive to be used other than on a few high value assets. Consequently, the present practices of assessing anchorage quality and performance are limited, time consuming or destructive [4].

In the mining industry rock bolts have been used increasingly in the last four decades and have become the primary support system. [5,6] They have been proved to reduce the number of fatalities due to roof fall accidents [7]. In a mine environment the anchor head consists of the bearing plate and the nut for applying the desired load which in turn provides the roof support. The design of the bearing plates for rock bolts is therefore significant due to their role of providing this roof support. Cincilla and Tadolini indicated that a well-designed bearing plate helps in resisting roof movement in the lower 0.6 m of the roof [8, 9]. Studies undertaken by Villaescusa et al. [10] showed that the geometry i.e. thickness and shape of the bearing plate has a significant influence in maintaining the load in the bolt especially after dynamic disruption such as blasting.

1.2. Non-destructive testing

Due to the high number of anchorages and rock bolts installed throughout the years an economical and effective method for monitoring their conditions is required to determine whether the installation has experienced any damage and has lost its reliability. A number of non-destructive testing methods (NDT) have been developed. These are based mainly on ultrasonic methods (using piezo-electric transducers) [11,12], guided ultrasonic methods [13], acoustic emission [14] or electromagnetic techniques [15]). All the NDT methods have merits, but also disadvantages. The ultrasonic based methods are generally only applicable to bolts and require the end of the bolt to be prepared to ensure good coupling between the transducer and the bolt, while the electromagnetic techniques have limited applicability dependent on rock type. Acoustic emission, while good for identifying ongoing cracking, requires near continual monitoring and again good coupling to the bolt. None of these methods are suitable for providing an estimate of the load in the bolt and all have very limited usage in the industry.

Research undertaken to address the need for a new method of anchorage assessment which provides estimation of the load in the anchorage, led to the development of a non-destructive

testing method, GRANIT (GRound ANchorage Integrity Testing). GRANIT operates by using a specially designed impact device [16]. The device applies an impulse load of small amplitude which effectively excites the natural frequencies of the system. The response of the anchorage is then measured by an accelerometer mounted on the device and recorded by a laptop computer. This response is then analysed in the frequency domain and compared to reference spectra obtained for different load levels from a datum anchorage of the same configuration. (Figure 2)

The GRANIT system estimates load in an anchorage by relating the shift in frequency obtained to the different load levels. In order to determine which part of the anchorage system influences most the dynamic behavior of the anchorage system and the shift in frequency, a lumped parameter model was used to investigate this. This model developed previously by Ivanovic et al [17] (Fig 1b) found that the stiffness of the anchorage head is the most influential part for detection of load.

1.3. Lumped parameter model

The model consists of masses, connected with springs and dash-pots, each representing a different part or interface within the anchorage system. The masses are calculated from the volume and density of each element, the axial stiffnesses k_i of the bar and the affected rock mass are calculated using the Hooke's law while the shear stiffnesses are calculated using plate theory according to [18]. The damping terms are functions of the mass, stiffness and an experimentally obtained damping coefficient [17]. The anchor head in the model consists of a mass representing the nut and the bearing plate and a single non-linear stiffness representing the combined stiffness of the bending of the plate and the effects of the interface between the plate and the rock. The stiffness of this interface is defined as $k_{bp.}$ This stiffness, required as an input for the lumped parameter model, is measured on an anchor head test rig through a test procedure reported previously [19]. The results from these tests give the load-displacement curve between the bearing plate and concrete surface in the form of a polynomial equation

$$F = ax^3 + bx^2 + cx + d \quad (1)$$

In the tests, two cycles of increasing and decreasing load were undertaken (see Figure 2). Localised crushing of the concrete surface accounts for the distance between the start point and the end

point of the first cycle which results in the non-recoverable deflection. No additional effective plastic deformation is noticed after application of the second cycle, which is therefore taken for reference in the stiffness computation.

The natural frequencies of the systems are calculated in the model, for different load levels, by an Eigenvalue analysis using a local linearization of the nonlinear head stiffness. The equivalent linear stiffness of the head k_{bp} is calculated for each load level by using the tangent stiffness at that particular load (Figure 3). This is obtained by differentiating the load/displacement curve (eq 2) to give

$$k_{bp} = 3ax^2 + 2bx + c \qquad (2)$$

and substituting in the displacement corresponding to the required load. The model allows the dynamics of the system to be replicated effectively and more computationally efficiently than if the whole system was simulated by means of, for example, FE modelling.

As an initial stage in the investigation, the variations of fundamental frequency were explored, by changing the stiffness ratio of the head, k_{hp}, relative to the stiffness of the free length of the steel tendon k_{bolt}. The aim was to ascertain what range of stiffness ratio of head to bolt is required to provide good load estimation. The results are shown in Figure 4 and are expressed in terms of *r,* the ratio between anchor head stiffness (k_{bp}) and the stiffness of the free length of the steel tendon (k_{bolt})

$$r = \frac{k_{bp}}{k_{bolt}} \qquad (3)$$

where $k_{bolt} = \frac{AE}{l_{free}}$, *A* is the cross section area of the tendon, *E* is the Young's modulus of steel and l_{free} is the free length of the anchorage. The percentage of frequency change is calculated with reference to the frequency of the non-loaded anchorage. [20]

The frequencies measured are controlled primarily by the stiffness of the tendon and local (tangent) stiffness of the anchor head at a particular load level [17]. Consequently, the greater the variation in stiffness over the load range, the greater the shift in frequency and so the more accurately the load can be estimated. However, if the head stiffness is initially very large in comparison to that of the tendon, then further increases in stiffness, with load, have little effect on the frequency and load estimation becomes inaccurate. From Figure 4 it can be seen that the frequency changes noticeably for lower stiffness ratios ($r < 50$). For higher stiffness ratios ($r > 50$) the frequency change alters by a very small percentage, which is insufficient for effective estimation of the load.

This distinction governs whether estimation of the load is possible or not. It is clear that load estimation is restricted only to anchorages with lower stiffness ratios, r and therefore that any proposed design needed to provide stiffnesses within the range $r < 50$. In addition it would need a stiffness characteristic which was sufficiently progressive to differentiate loads.

The requirement to have a free length, l_{free}, to provide a tendon stiffness may appear restrictive, as many rock bolt systems will be designed to be fully grouted, as is the case with mining bolts. However, from studies undertaken in North Parks and other mines and in tunnels it is found that all bolts either develop free length during initial installation where the top end of the grouted length is not usually completely bonded [21,22] or in some civil engineering cases, it has been debonded by using a tape and then grouted. [23]

This paper presents the analysis undertaken to design a bearing plate for a tensioned rock bolt, which optimises the stiffness characteristic so that the dynamic response maximizes the effectiveness of the GRANIT system for load estimation while still providing the support required for the mining and construction industries. The novelty of the design compared to standard bearing plates is in its geometry which provides a prescribed nonlinear stiffness characteristic.

2. Plate design and analysis

In order to obtain a response from the GRANIT system which will indicate a change in load, the specification of a bearing plate for use with a typical mining rockbolt application includes: Low levels of plastic deformation, a progressive increase of stiffness with load and a load capacity up to 200kN.

To produce a design with these required characteristics a number of FE models of typical bearing plates placed on a concrete surface were modelled and modified incrementally using the Abaqus Standard software package v 6.10. [24]. It should be noted that Abaqus was used to perform a quasi-static analysis in order to investigate the flexibility of the bearing plate. The stiffness characteristics of the bearing plate obtained from these FE models were then used in the lumped parameter model to perform full dynamic simulations and monitor frequency shifts. A full nonlinear dynamic simulation was not required in Abaqus because the only dynamic load is the impulse applied by the impact device which is sufficiently small that the head stiffness is effectively within a linear regime during its application.

The FE models developed simulate direct contact between the bottom surface of the plate and the surface of the concrete (base). The contact was simulated, using a penalty contact method based on a Coulomb friction model together with the general contact algorithm in Abaqus/Standard. The penalty friction formulation is considered to work well for most static problems, including most metal forming applications and was therefore used in the simulations reported here.

Both friction and frictionless tangential interactions were applied at the interface between the plate and the concrete surface on which it was installed in order to understand how these influenced the system behaviour. Normal interaction was set as “hard contact”, which allows no inter-penetration of the parts during contact. For the case of normal friction, a friction coefficient, $\mu = 0.57$, was chosen for the dry contact between the steel and concrete surfaces, based on values reported in literature by Rabbat and Russell [25] while a friction coefficient, $\mu = 0.74$, was chosen for dry unlubricated contact between the steel surfaces. This was based on values reported by Grigoriev et al [26]. A number of plates were generated and analysed in order to obtain a shape that satisfied both the flexibility and load resistance requirements.

2.1. Square and circular plates of constant thickness

A square, commercially available plate, commonly used in the mining sector was analysed as a reference for further design simulations. A 3D FE model of this bearing plate was generated, with the dimensions: 140x140 mm and a uniform thickness of 7 mm and a 35 mm hole with the material properties of the steel of a Young’s modulus of 206 GPa and yielding limit of 600 MPa. A

rigid square block was created as the support surface taking into consideration that the initial aim was to characterise the stiffness of the plate as it was loaded, without allowing any deformation of the support surface.

For simplicity of computation, the top of the plate was fixed and the load was applied as a uniform pressure at the bottom of the block onto which the plate was installed. The load was increased from 0 to 200kN. The choice of holding the top of the plate fixed and applying the force to the block or holding the block fixed and applying the load to the top of the plate is arbitrary but the former was easier to implement in this case.

The resulting stress distribution at a load of 56kN is shown in Figure 5 from which it can be seen that the plate has reached its yielding limit at this load, and develops plastic deformation. At 170 kN the plate was found to have deformed plastically almost completely, in particular at the sides and the internal edge. It should be noted that in mining applications this flattening of the plate is often used to visually identify highly loaded bolts.

A circular plate, of the same primary dimensions and properties was then modelled to investigate whether it could withstand higher loads than the square plate before plastic deformations occurred. The results show that stresses are distributed axisymmetrically and the plastic limit is reached at 85 kN. However, a high stress concentration is evident around the edges of the inner diameter of the plate indicating that the plate thickness needed to be increased. (Figure 6). Neither design meets the criterion of minimising plasticity required for a good design.

2.2. Optimisation of a Plate for GRANIT Response

In order to achieve the load resistance combined with progressive stiffness a number of different geometries were further simulated in Abaqus. Since the flexibility of the plate is important, as is its ability to resist high loads, a series of plates was modelled where the cross section profile decreased from the interior to the outer edge. The plate in the model was supported by a block fixed at the base, a flat secondary plate was introduced on top of the plate in order to have an even surface, and a nut was used to apply the load to better replicate actual load conditions. As there are no other restraints, the plate can deform freely in all directions. The concrete part was

partitioned in order to refine the mesh in the area of contact and provide accurate results. The results showed that for this style of plate with a reducing thickness the area of contact between the plate the surface widens as the load increases. When a larger part of the surface is in contact, the bearing plate becomes stiffer, which in turn increases the frequency of the whole system. However, the upper profile of the bearing plate, also has an influence on the stiffness of the plate as the thickness of the central part of the plate has a larger influence at higher loads whereas the peripheral part has greater influence at lower loads. In other words, a decrease of the thickness of the peripheral part gives a decrease of frequencies at lower loads, while an increase of the thickness of the central part increases frequencies at higher loads. From the models tested it was possible to conclude that the frequency response is more dependent on the profile of the cross-section of the plate than on its diameter. Generally, an increase of the plate diameter results in a decrease in the natural frequency because the plate becomes more flexible overall.

Producing a detailed 3D model is computationally expensive and therefore a comparison with 2D axisymmetric models was undertaken. The results proved the 2D model to be accurate, while providing the same response in a much quicker time scale. In addition, an axial symmetric model allowed the production of a much finer mesh, potentially giving better accuracy especially around the contact region. A comparison of the load/displacement curves, shown in Figure 7 indicates that there is no significant difference between the 3D and the 2D axisymmetric models. The results proved the models to be equivalent also in terms of the level of displacement, strain and stress and justified the choice of 2D axisymmetric model to be used in further analysis.

3. Cyclic loading analysis

One of the requirements for the anchor plate was to limit plastic deformation as this could affect its stiffness characteristic (as can be seen in Figure 3). However, it was postulated that if the stresses in the plate exceeded the yielding point during the first loading only, the plastic deformations could be tolerated. A series of loading/unloading cycles were therefore simulated to ensure that no further plastic deformation or fatigue occurred within the plate following the load cycles.

Taking all the previous findings into account, the final bearing plate proposed has a 3 mm thickness at the exterior edge and the thickness increases progressively towards the inner edge. The total height of the plate is 16 mm and the external diameter measures 140 mm. Figure 8 shows a comparison of the new plate cross section profile with that of the standard plate which was used as the initial reference for the study. This profile which results in the required stiffness characteristics is the novel aspect of the plate.

To verify that no appreciable deformation of the concrete is present, the supporting block in the FE simulation was then also simulated as a deformable part with elastic resistance of 35 MPa and Young's modulus of 35GPa. During the loading, two surface interactions take place, one at the contact between the plate and the supporting block and the other at the contact between the nut and the plate, both of which are investigated by varying the friction coefficient.

Two models were created to evaluate the importance of the friction at the interfaces. These were:

(i) the steel-concrete interaction used a friction coefficient of 0.57, with the steel-steel contact 0.74

(ii) a friction coefficient of 0.04 was used at both the contact between the plate and the concrete and at the contact between the nut and the plate. This value simulates a low friction/lubricated surface e.g. a Teflon coated surface which could be used to mitigate any hysteresis resulting from stick/slip at the interfaces.

To evaluate the effect of yielding, four load-unload cycles (0-200-0kN) were undertaken for each scenario.

3.1. Friction model, datum case

FE results

The results show that for the datum case the first load curve is quite different from the subsequent cycles (Figure 9). Plastic deformations spread within the model more consistently than in previous simulations, which is in accordance with expectations. However, after the first load phase, the stress is always found to be below the steel yielding point. Figure 10a shows the plastic strain measured at the point highlighted on the mesh (Figure 10b). There is very little plastic deformation after first cycle as can be seen at the points at 7s, 10 and 12s where the load

cycles reverse. The contact area progressively increases with increase of load and the bearing plate is completely in contact with the supporting block at the 200 kN load level.

The plate stiffness was obtained from the data, and indicated that the stiffness increases by almost 200 times from 0 to 200 kN load. At the 0 kN load, a difference in stiffness between the load phase and the unload phase of 9.6% was found. At 200 kN load, the difference in stiffness between the loading phase and unloading phase becomes 52.6%. This difference present between the same load level in the load and unload phase is caused by the friction acting at the bottom of the bearing plate. The surfaces do not slide freely on the horizontal plane, but are restrained partially by friction. This is discussed later.

Lumped parameter model results

In order to observe how the stiffness characteristics of the anchor head influence the overall frequency anchorage response, the lumped parameter model was set up using the material and geometry properties of the anchorage system utilised in previous laboratory tests [27]. This had a free length of 400 mm, fixed length of 2100 mm, protruding length of 100 mm, bolt diameter of 25 mm and Young's modulus of steel of E = 206 GPa. The model parameters are given in Table 1. The plate stiffness characteristics obtained from Abaqus were included in the model and the frequency response of the anchorage determined for four loading cycles (0 to 200 kN), as shown in Figure 11.

Figure 11 shows that the overall frequency shift is greater than 2000Hz for the 200 kN load variation. Over the range 0-100 kN the average gradient is approx 15 Hz per kN. In the GRANIT system, sampling of the data is usually undertaken at 20kHz with 4000-10,000 samples collected which provides a resolution of between 2 Hz and 5Hz in the frequency domain. For any change to be detected, it therefore needs to result in a frequency shift larger than 5 Hz. A shift of 15 Hz per kN therefore provides a very useable sensitivity for load estimation. In a real situation, pre-loading the plate up to 200 kN prior to using it would have advantages as the plastic deformations would have taken place and a quasi-elastic response would result in subsequent cycles.

A change between the first and the subsequent loading phases can be clearly seen in the figure where, with every loading phase, the difference between each subsequent loading cycle

decreases. This is different from the unloading cycles, which all seem to be consistent. The frequency corresponding to a load of 200 kN can be seen to be different on the loading cycle and on the unloading cycle. This discontinuity results from the differentiation of the load-displacement curve to give the stiffness, and it is possible to explain this by the presence of friction. On loading, the friction resists the movement of the plate as it tries to expand and slide over the supporting surface. On releasing the load, the friction again resists motion but in this case resists the elastic recovery to the original state. From the perspective of estimating load by using the frequency, designing the system so that the loading and unloading curves are as close as possible reduces the chance of errors. To reduce the distance between the two curves the friction in the system should be minimised. For frictionless contact all the curves should be the same after the initial plastic deformation of the plate.

3.2. Friction model, reduced friction

FE results

In order to investigate this effect and whether the use of a low friction surface at both contact interactions could result in a smaller difference between the different loading cycles, a series of simulations was undertaken with low friction. In this model, Teflon layers were introduced between the plate and the concrete and between the nut and the plate. This was simulated by reducing the friction coefficient to 0.04 at both contacts.

The resulting loading and unloading curves, shown in Figure 12, indicate that the substantial difference between cycles, found in the cases of higher friction, decreases with the reduction of friction between interfaces.

Lumped parameter model results

The stiffness characteristics of these cycles were again included in the model and the results obtained are shown in Figure 13. As found in the model with higher friction it is clear that the first cycle trend is still different from the subsequent ones. However, it can be seen that all other loading-unloading curves are superimposed almost perfectly up to 120kN while with the higher friction (Figure 11) there was a difference of approx. 120Hz at this load. Although there would be

less accuracy for load prediction in the range 120-200 kN, for typical bolts a load of 180kN/200kN would be treated as highly stressed and in practice would be followed up with some remedial actions anyway and so an indication that a bolt has exceeded a certain level may be sufficient.

4. Commissioning/ Validation of the plate

In order to further confirm the validity of the proposed plate design a series of static and dynamic physical tests were undertaken and compared to the results from numerical simulations.

4.1 Static experimental and ABAQUS load displacement testing of the plate

The plate described was manufactured and tested in the laboratory in order to measure the actual load – displacement behaviour and validate the simulations. The prototype was manufactured using steel with a yield strength of 319 MPa. It was tested using an Instron 8500 testing machine, with the plate placed against a concrete block of 300 mm diameter, and the vertical displacement between the loading head of the Instron and the concrete surface measured using two LVDTs (RDP D5/200AG) to give the true load-displacement curve (Figure 14). This form of measurement provides the correct stiffness of the plate and interface with no effects from the stiffness of the testing machine or the concrete block. The load was cycled two times, from 0.5 up to 200 kN and back to 0.5 kN. For comparison, the same configuration was simulated in ABAQUS.

The results show good correlation between tests and simulations in the 0-200kN load range. The laboratory tests (Figure 15) showed a clear difference between the first load cycle and consequent cycles as was noticed in the FE simulations. The shapes of the curves obtained from the tests and ABAQUS simulations appear to be similar, although the initial non-recoverable deformation during the first load cycle is slightly larger in the laboratory experiments compared to the ABAQUS simulation. This is thought to be due to the localised crushing of small asperities on the concrete surface in the experiment; a situation which did not occur in the model as the surface is perfectly flat.

4.2 Dynamic testing and simulation of a test anchorage with the plate

The plate load-displacement test results were used as input for the lumped parameter model described earlier. The stiffness results from tests were somewhat scattered, and therefore in order to plot a reasonably well-shaped curve, a logarithmic trend line was generated in the displacement/load graph. This was then differentiated with respect to force to give flexibility. The result was then inverted to give the stiffness as a function of load, expressed as

$$k_{bp} = 11.402\ F - 8.047$$

where F is the vertical load (in N) and k_{bp} is the stiffness of the bearing plate (in N/m). This expression shows a linear relation between stiffness and load. For comparison, the equivalent load displacement graph for this curve fit is shown in Figure 15 alongside the test curve. The offset along the longitudinal axis does not affect the stiffness calculated from the curve.

In order to validate the results from the lumped parameter model, physical testing was also undertaken on a small laboratory anchorage shown in Figure 16. This anchorage had protruding, free and fixed lengths of 200 mm, 500 mm and 150 mm respectively, a bolt diameter of 25 mm, a 28 mm bore hole and outer diameter of the concrete of 300mm. This anchorage was tested using the GRANIT test which has previously been employed successfully on bolts of this size. The results obtained from the tests are shown along with the corresponding model results in Figure 16. The simulated anchor system has the same geometry and material properties as those used in the laboratory tests and uses the material properties presented in Table 2. The GRANIT impact device is represented in the model as a mass of 2.2 kg attached to the protruding length, the bearing plate, the nut and the plate beneath as a mass of 2.7 kg.

Figure 17 shows a shift of approximately 1.3kHz for the proposed bearing plate over the 0-200 kN load range with the GRANIT system. When compared with the simulations, using the same geometry, it appears that the frequencies from the experimental data are consistently higher compared to those for the corresponding load levels obtained from numerical simulations. This is

unusual as more flexibility would generally be expected in the experimental rig. This suggests that friction may have a larger than expected effect in restricting the movement of the plate in the experiment, resulting in a slightly higher stiffness. However, the overall results indicate that the anchorage, with the inclusion of the newly designed bearing plate, which has been patented [28], is amenable for regular GRANIT testing and provides a good level of load discrimination.

5 Conclusions

This paper presents the results of both experimental and numerical studies into the effect of anchor head stiffness on the vibration response of rock bolt. The aim was to design a bearing plate that could provide prescribed changes in head stiffness with load, thus providing measurable changes in frequency and ultimately allowing for effective non-destructive load estimation. In particular, the aim was to provide a method of modifying those anchorages where the principal frequency does not shift with increasing load and therefore estimation of load is not straightforward. A suitable design, which improves the load estimation capability of the GRANIT system has been achieved. The results from the FE simulations and subsequent lumped parameter model show that the introduction of this specifically designed plate can modify the overall anchor head characteristics, allowing the stiffness ratio between the head and the anchor to vary consistently within the workload range. This variation in stiffness ratio leads to a consistent increase of principal frequencies of the anchorage system associated with the increase of load. Care is however required in mitigating the effects of friction at the interfaces between the plate and the rock surface, as this reduces the reliability of the load estimate. The results obtained from the full-scale experiments indicate that the plate design is a viable solution for load-estimation in anchorage systems and could be implemented in practice.

References

[1] BSI (1989) 8081: 1989 British Standard Code of Practice for Ground Anchorages. BSI, London, UK.

[2] BSI (1996) 7861:Part 1:1996 Strata reinforcement support system components used in coal mines . BSI, London, UK.

[3] Littlejohn S and Mothersille D (2008) Maintenance and monitoring of anchorages: guidelines. Proceedings of the Institution of Civil Engineers - Geotechnical Engineering **161(2):** 93–106.

[4] Zou DHS (2004) Analysis of in situ rock bolt loading status. International Journal of Rock Mechanics and Mining Sciences **41(3)**: 762-767.

[5] Whitaker A. (2001) Critical Assessment of Past Research into Rock Bolt Anchorage Mechanisms. University of New South Wales Mining Research Centre, Sydney. UMRC Research Report RR3/01.

[6] Hebblewhite BK and Lu T (2004) Geomechanical behaviour of laminated, weak coal mine roof strata and the implications for a ground reinforcement strategy. International Journal of Rock Mechanics and Mining Sciences **41(1)**:147-157.

[7] Smelser TW, Dar SD, Pettibone HC and Bolstad DD (1982) Modeling and Field Verification of Roof-Bolt Systems. Society of Mining Engineering. AIME preprint, pp. 82- 121.

[8] Cincilla WA and Tadolini SL (1986) Effects of bearing plates and grout column length on resin-bolt performance. In *Proceedings of SME Symposium on Engineering Health and Safety in Coal Mining*, SME, Littleton, USA, pp.60-74.

[9] Tadolini SC and Ulrich BF (1986) Evaluation of Bearing Plates Installed on Full-Column Resin-Grouted Roof Bolts. U.S. Department of the Interior, U.S. Bureau of Mines. RI 9044,, pp. 27.

[10] Villaescusa E, Varden R and Hassell R. (2008) Quantifying the performance of resin anchored rock bolts in the Australian underground hard rock mining industry. International Journal of Rock Mechanics and Mining Sciences **45(1):** 94-102.

[11] Thurner HF (1979) Non destructive test method for rock bolts. In *Proceedings of International Congress on Rock Mechanics*, Montreux, Switzerland, Vol3, pp. 254-255.

[12] Wittenberg D and Ruppel U, Quality Management for Grouted Rockbolts (2000) In *Proceedings of the 19th International Conference on Ground Control in Mining*, Morgantown, WV, West Virginia University,USA, pp. 249-254.

[13] Beard MD and Lowe MJS. (2003) Non-destructive testing of rock bolts using guided ultrasonic waves. International Journal of Rock Mechanics & Mining Sciences **40(4)**: 527–536.

[14] Robert JL and Brachet-Rolland M (1982) Survey of Structures by Using Acoustic Emission Monitoring, IABSE (International Association For Bridge and Structural Engineering) Symposium, Washington D.C., Maintenance, Repair and Rehabilitation of Bridges, Final Report, IABSE Reports, Vol 39, pp. 33-38

[15] Bigby D N & Arthur J (2001) Improved Rockbolting Safety Worldwide through Recent UK Instrumentation and Testing RTD. International Symposium on Roofbolting in Mining, RWTH, Aachen, Germany. pp 463-480.

[16] Neilson RD, Ivanovic A, Starkey AJ and Rodger AA (2007) Design and dynamic analysis of a pneumatic impulse generating device for the non-destructive testing of ground anchorages. Mechanical Systems and Signal Processing, **21(6)**, 2523–2545.

[17] Ivanovic A, Neilson RD and Rodger AA (2002) Influence of Prestress on the Dynamic Response of Ground Anchorages, Journal of Geotechnical and Geoenvironmental Engineering, **ASCE 128(3)**, 237-249.

[18] Young WC (1989) *Roark's Formulas for Stress and Strain*. Sixth Ed., McGraw-Hill Book Company**.**

[19] Ivanovic A and Neilson RD (2008) Influence of Geometry and material properties on the axial vibration of a Rock Bolt, International Journal of Rock Mechanics & Mining Sciences **45(6)**, 941–951.

[20] Starkey A, Ivanovic A, Neilson RD and Rodger AA (2003) Using a Lumped Parameter Dynamic Model of a Rock Bolt to Produce Training Data for a Neural Network for Diagnosis of Real Data. Meccanica **38(1)**, 131–142.

[21] Neilson, R. D., Rodger A.A., Ivanović, A, Starkey, A. J., Chappell M., Jackson B. H. and Ritson A (2004), Rock/Cable Bolt Integrity Testing using GRANIT – Recent Field Applications, 5th International Colloquium on Roofbolting in Mining, Aachen, pp. 523-528.

[22] Neilson, R. D., Ivanović, A, Starkey, A. J. and Rodger A.A., (2004) Quality Control in Rock

Bolt Installation, 5th International Conference on Quality, Reliability and Maintenance, Oxford, UK, pp79-82

[23] Rodger, A.A. Littlejohn, G.S., Holland D.C. and Xu, H. (1993), Dynamic response of rock bolt systems at Pen y Clip in North Wales, Options for Tunnelling, Developments in Geotechnical Engineering, **74**:719-727.

[24] Abaqus/CAE User's Manual (Version 6.10)) https://www.sharcnet.ca/Software/Abaqus610/Documentation/docs/v6.10/books/stm/default.htm

[25] Rabbat BG and Russell HG (1985) Friction Coefficient of Steel on Concrete or Grout. Journal of Structural Engineering, **ASCE 111(3)**, 505–515 DOI: 10.1061/(ASCE)0733-9445(1985)111:3(505)

[26] Grigoriev IS, Meilikhov EZ and Radzig AA (1996). *Handbook of Physical Quantities.* Boca Raton: CRC Press, 145-156.

[27] Ivanović A and Neilson RD. (2013) Non-destructive testing of rock bolts for estimating total bolt length. International Journal of Rock Mechanics and Mining Sciences, **64(1)**, 36-43. DOI: 10.1016/j.ijrmms.2013.08.017

[28] Patent Application PCT/BG2005/003254, (2002) Improved Anchorage Head Assembly applied for by the University of Aberdeen and Amec Group Ltd., Inventors: R D Neilson, AJ Starkey, A Ivanović, B H Jackson, A J Ritson.

Parameter	Description	Value
$m_{rb,pr}$	mass of rock bolt along the protruding length	0.385 kg
$m_{rb,\ free}$	mass of rock bolt along the free length	1.541 kg
$m_{rb,\ fixed}$	mass of rock bolt along the fixed length	7.321 kg
$m_{rm,free}$	mass of rock mass along the free length	56.712 kg
$m_{rm,fixed}$	mass of rock mass along the fixed length	269.384 kg
$k_{rba,pr}$	stiffness of the rock bolt (axial) along the protruding length	1.016 GN/m
$k_{rba,\ free}$	stiffness of the rock bolt (axial) along the free length	25.403 MN/m
$k_{rba,\ fixed}$	stiffness of the rock bolt (axial) along the fixed length	53.479 MN/m
k_{bps}	stiffness of the bearing plate	185.548 MN/m
k_{g}	stiffness of grout	411.018 GN/m
$k_{rma,free}$	stiffness of the rock mass (axial), along the free length	6.193 GN/m
$k_{rma,fixed}$	stiffness of the rock mass (axial), along the fixed length	1.304 GN/m
$k_{rma,free}$	stiffness of the rock mass (axial), along the free length	65.016 GN/m
$k_{rma,fixed}$	stiffness of the rock mass (axial), along the fixed length	308.825 GN/m
$c_{rba,pr}$	damping of the rock bolt (axial), along the protruding length	11.872 kNs/m
$c_{rba,free}$	damping of the rock bolt (axial), along the free length	11.872 kNs/m
$c_{rba,fixed}$	damping of the rock bolt (axial), along the fixed length	11.872 kNs/m
c_{bps}	damping of the bearing plate	40.765 kNs/m
c_{g}	damping of the grout	7.632 kNs/m
$c_{rma,free}$	damping of the rock mass (axial), free length	17.779 kNs/m
$c_{rms,free}$	damping of the rock mass (shear), free length	57.608 kNs/m
$c_{rms,fixed}$	damping of the rock mass (shear), fixed length	273.636 kNs/m

Table 1

Properties	Resin	Concrete	Steel
Density (kg/m^3)	1825	2440	7895
Compressive strength (MPa)	80	90.1	-
Young's modulus (GPa)	12	35	207
Poisson's ratio	0.383	0.15	0.3

Table 2

Figure Captions

Figure 1a Schematic diagram of a complete ground anchorage system

Figure 1b Lumped parameter model

Figure 2 Schematic diagram of the GRANIT system

Figure 3 Load - displacement curve of a bearing plate

Figure 4 Frequency change with stiffness ratio

Figure 5 FE analysis results of a 7mm thick square bearing plate

Figure 6 FE analysis results of a 7mm thick circular bearing plate

Figure 7 Comparison of load - displacement curves of the 3D and the 2D axisymmetric models.

Figure 8 Comparison between the profiles of a commercially available plate and the newly designed bearing plate

Figure 9 Load - displacement results obtained from the FE analysis of the cyclic loading on the new plate using the friction model

Figure 10a Plastic strain measurements in the new plate using the friction model

Figure 10b FE analysis showing the point at which the plastic strain obtained in Fig 10a was measured

Figure 11 Frequency - load relationship for the friction model: lumped parameter results

Figure 12 Load - displacement curve for the reduced friction model: FE results

Figure 13 Frequency - load relationship for the reduced friction model: lumped parameter results

Figure 14 Laboratory test on the bearing plate to measure the actual load – displacement behaviour

Figure 15 Comparison of the load - displacement curves of the load test and the FE results

Figure 16 Physical testing on a small laboratory anchorage

Figure 17 Comparison frequency - load relationship for the test and simulation results

Figure 1a

Click here to download Figure Figure 1a.jpg

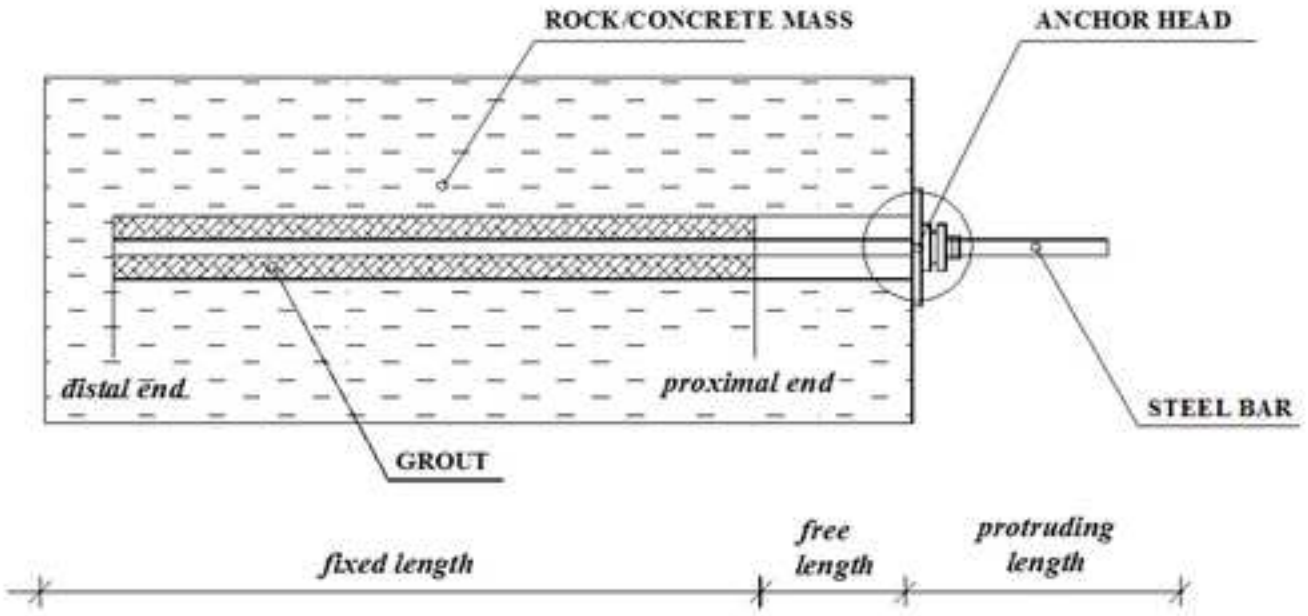

Figure 1b

Click here to download Figure Figure 1b.jpg

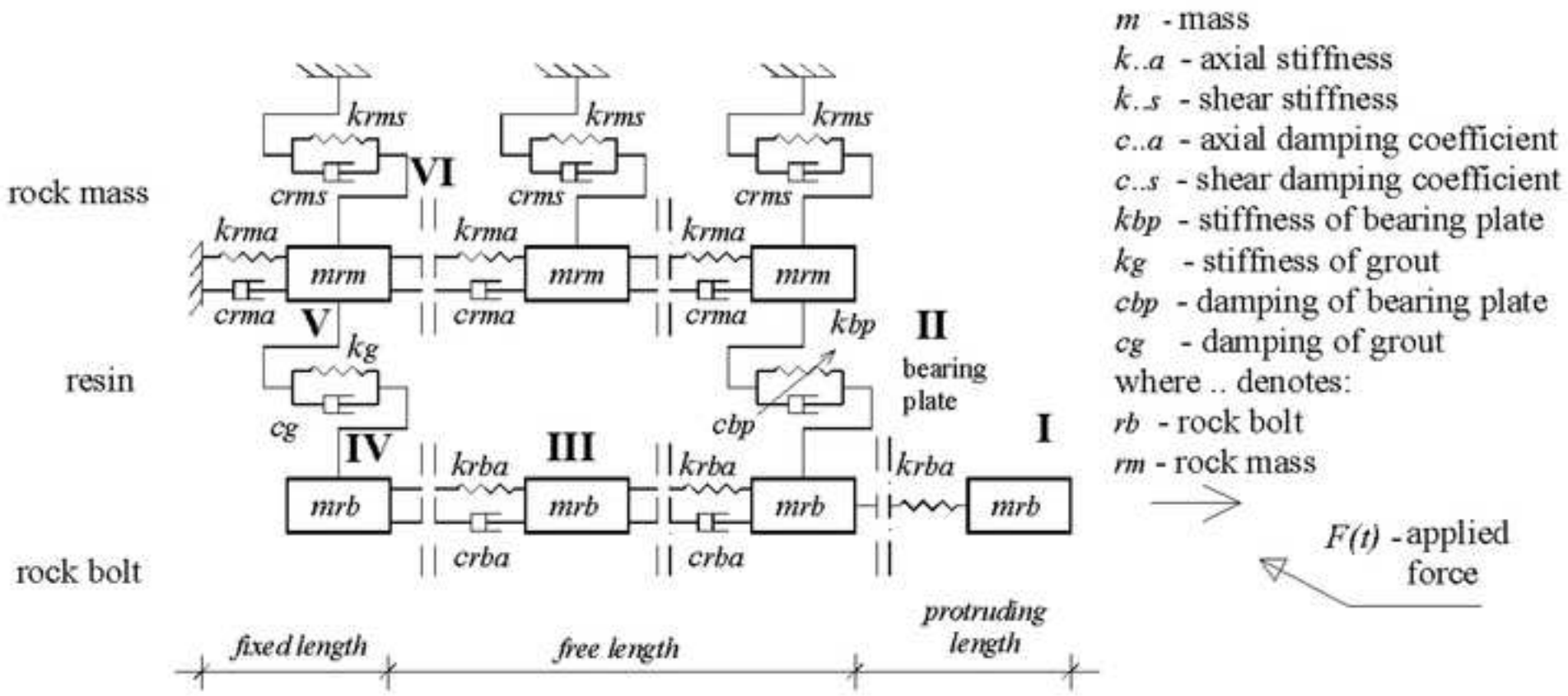

Figure 2

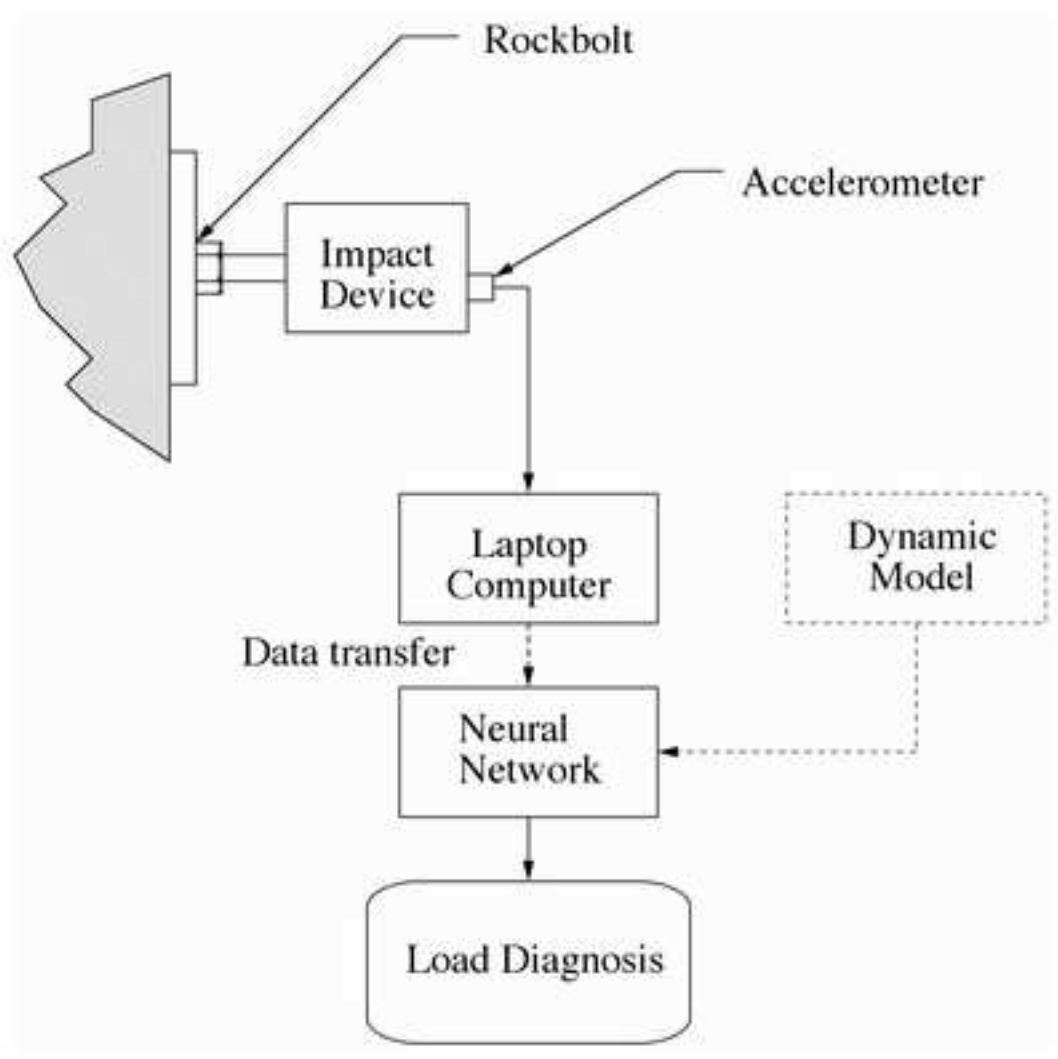

Figure 3

Click here to download Figure Figure 3.jpg

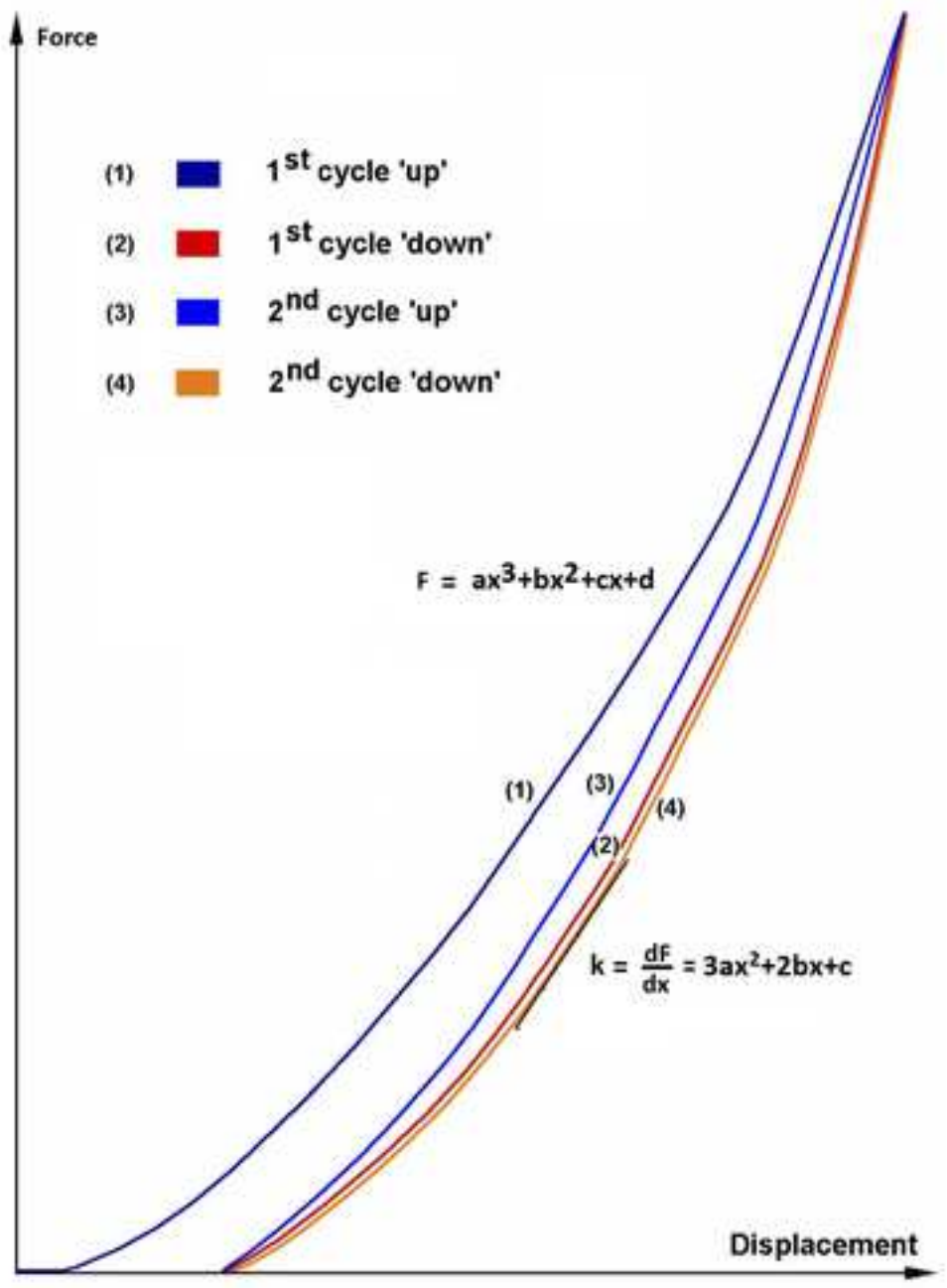

Figure 4

Click here to download Figure Figure 4.jpg

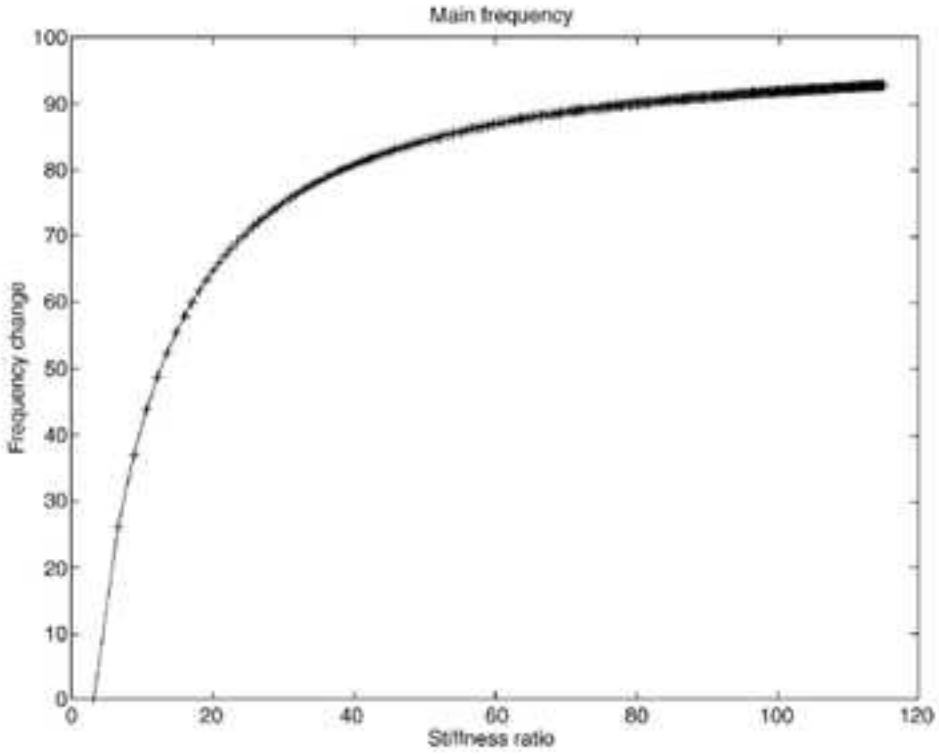

Figure 5

Click here to download Figure Figure 5.jpg

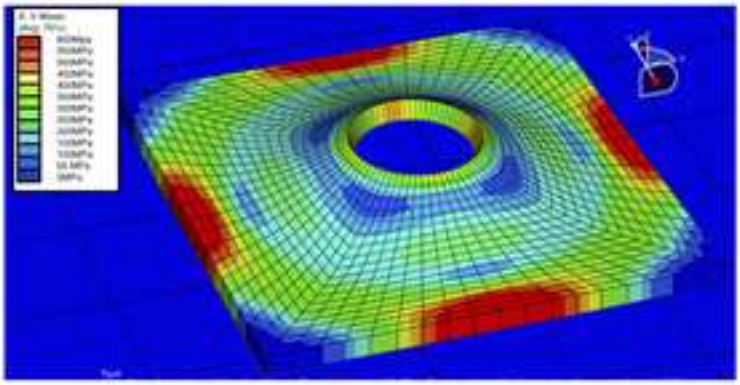

Figure 6

Click here to download Figure Figure 6.jpg

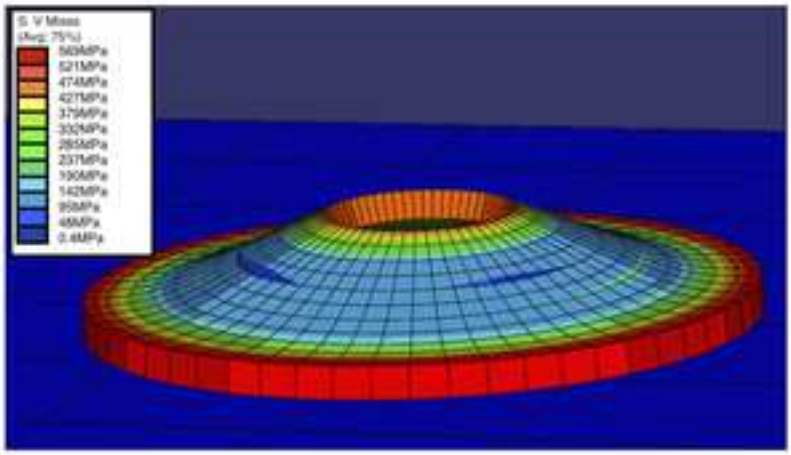

Figure 7

Click here to download Figure Figure 7.jpg

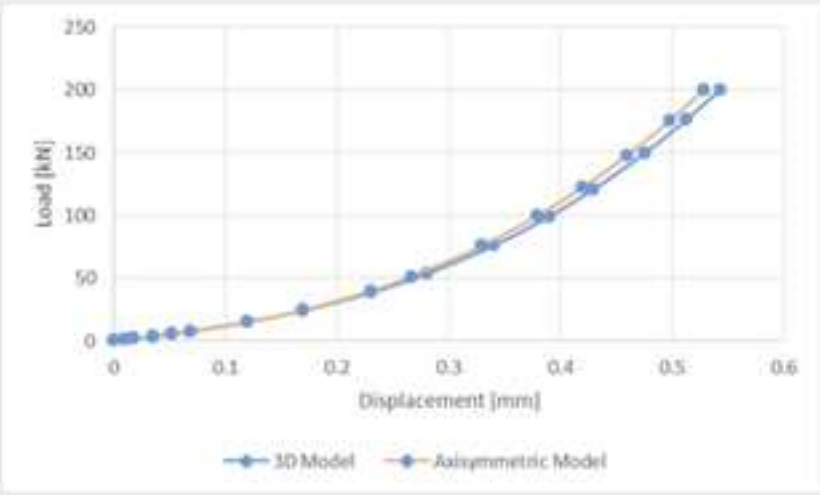

Figure 8

Click here to download Figure Figure 8.jpg

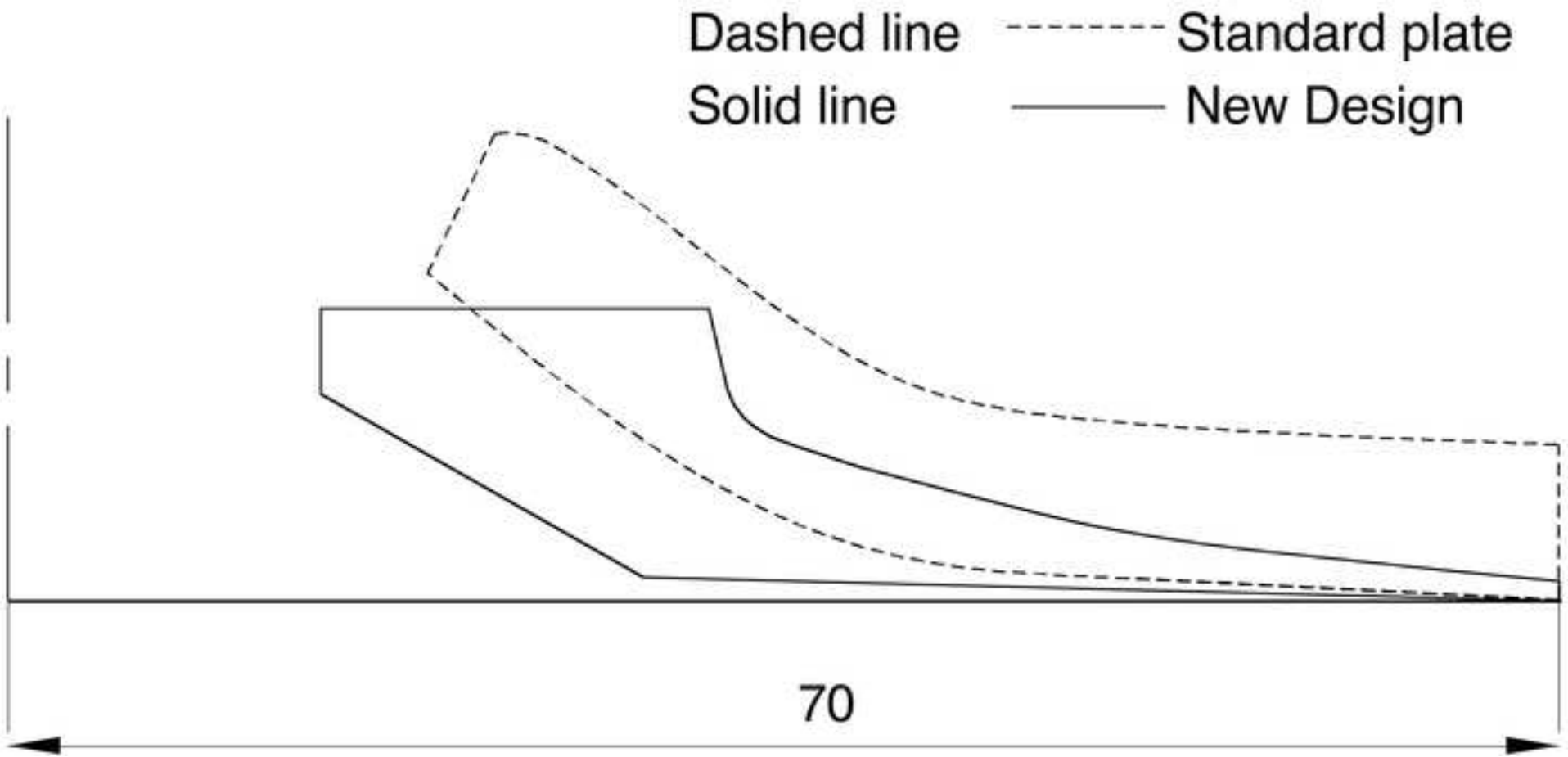

Figure 9

Click here to download Figure Figure 9 Edited.jpg

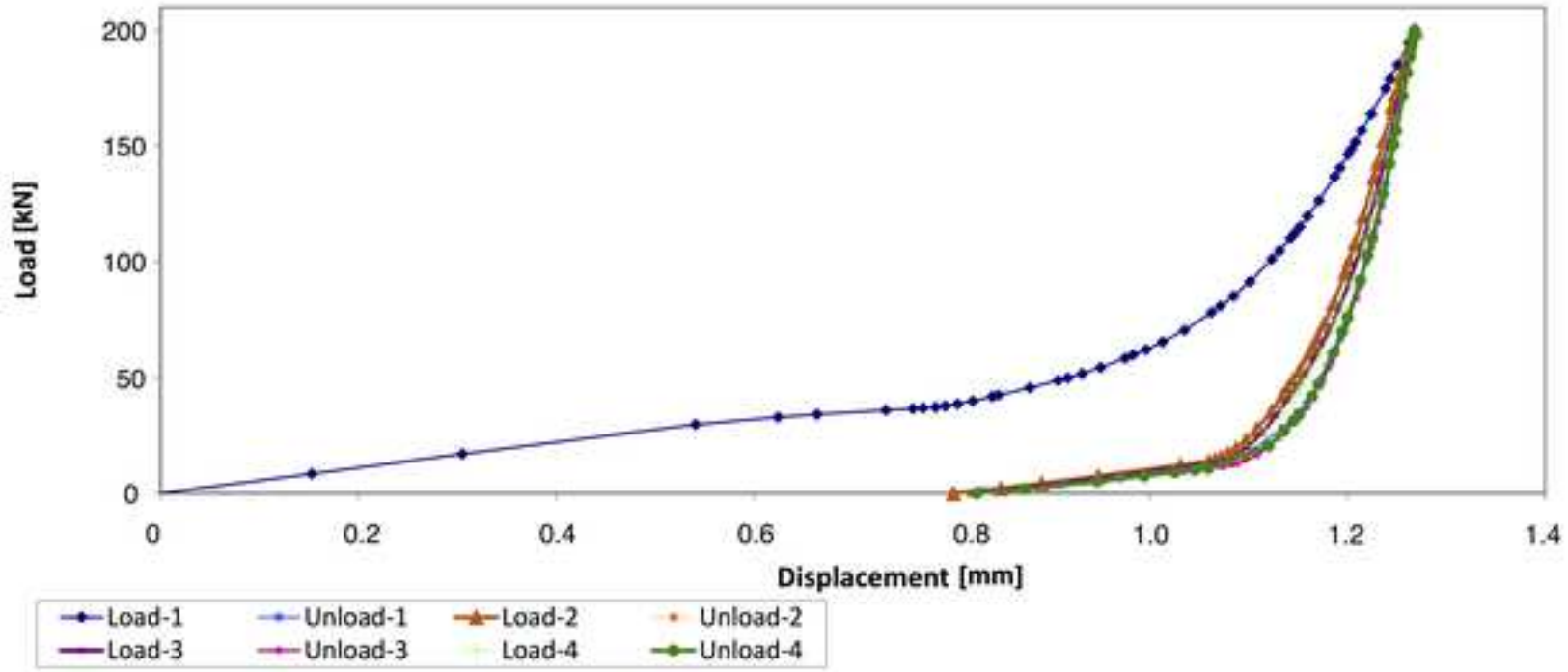

Figure 10a

Click here to download Figure Figure 10a.jpg

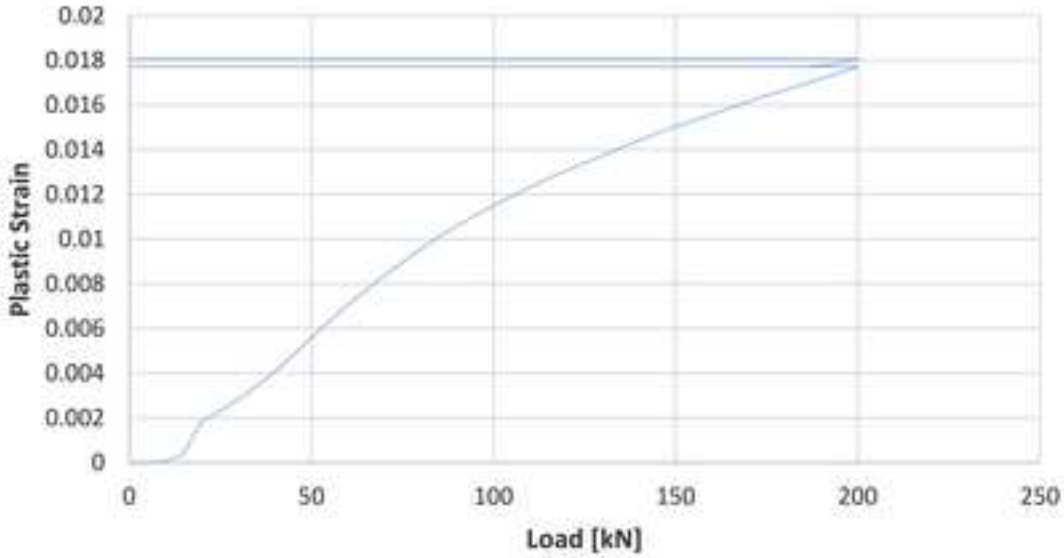

Figure 10b

Click here to download Figure Figure 10b.jpg

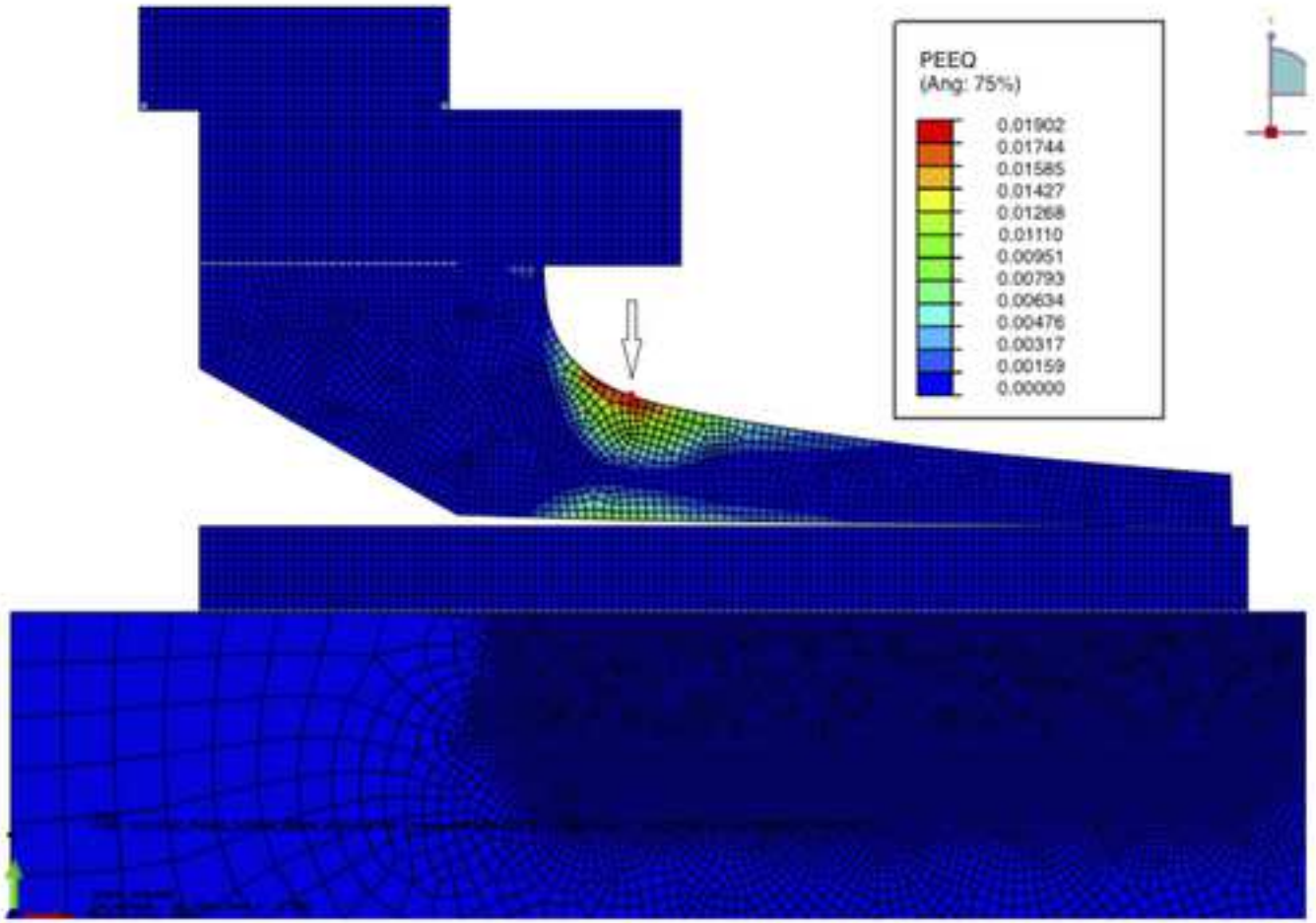

Figure 11

Click here to download Figure Figure 11 Edited.jpg

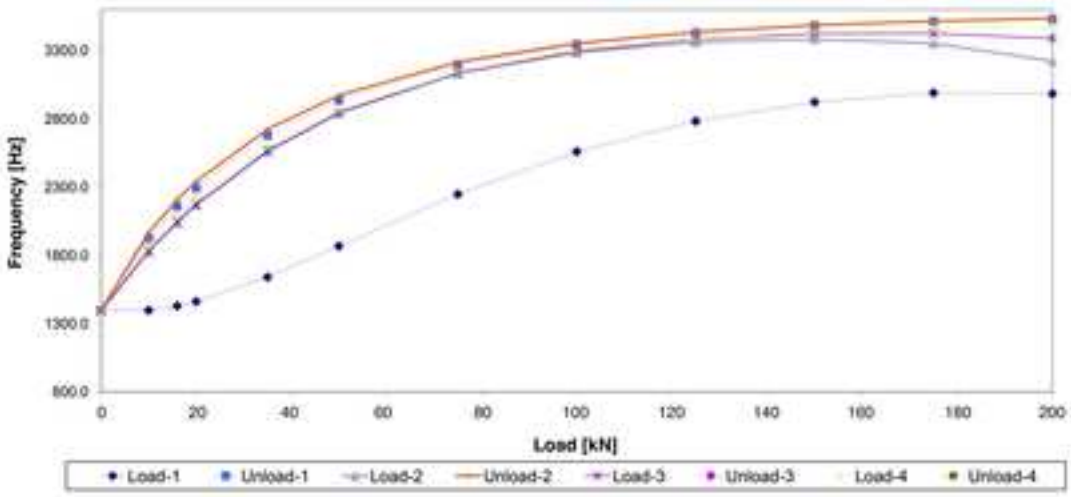

Figure 12

Click here to download Figure Figure 12 Edited.jpg

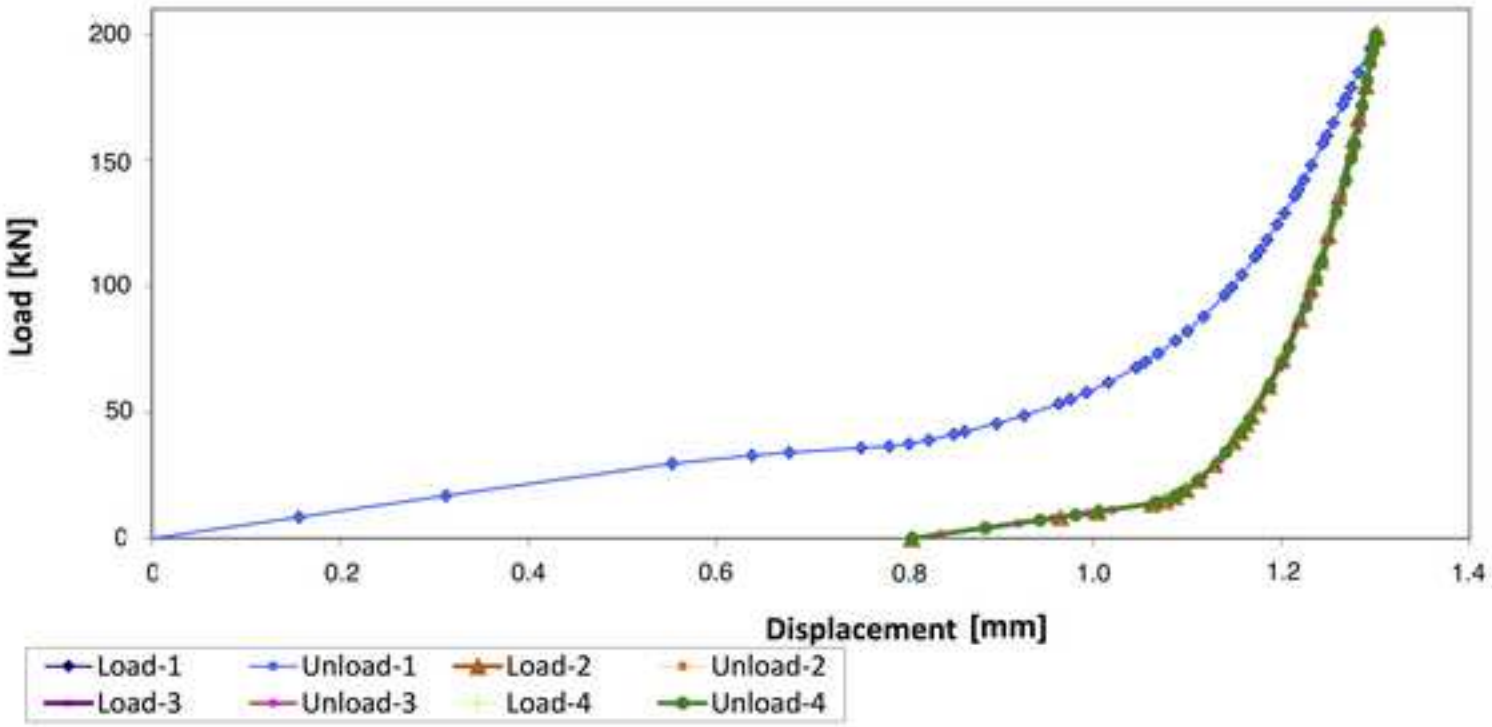

Figure 13

Click here to download Figure Figure 13 Edited.jpg

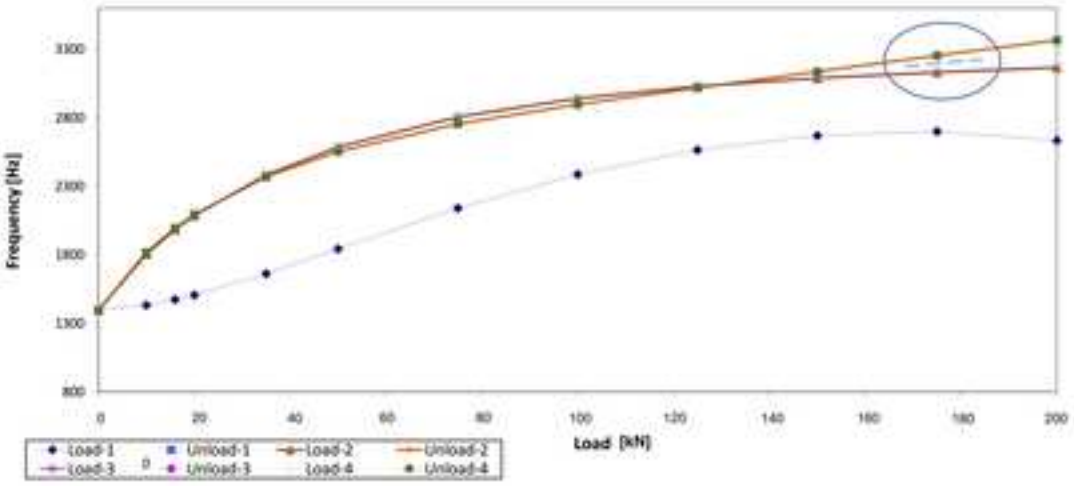

Figure 14

Click here to download Figure Figure 14.jpg

Figure 15

Click here to download Figure Figure 15.jpg

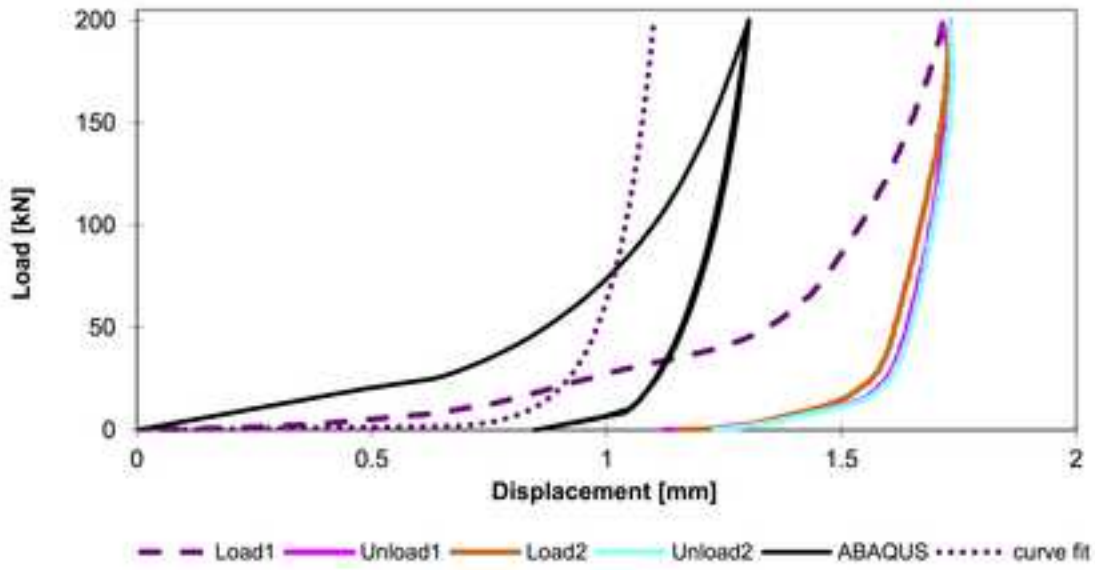

Figure 16

Click here to download Figure Figure 16.jpg

Figure 17

Click here to download Figure Figure 17.jpg